JACS
JOURNAL OF THE AMERICAN CHEMICAL SOCIETY

pubs.acs.org/JACS

Communication

# Simultaneous Quantification of Vesicle Size and Catecholamine Content by Resistive Pulses in Nanopores and Vesicle Impact Electrochemical Cytometry

Xin-Wei Zhang, Amir Hatamie, and Andrew G. Ewing*

Cite This: J. Am. Chem. Soc. 2020, 142, 4093−4097

Read Online

ACCESS | Metrics & More | Article Recommendations | Supporting Information

**ABSTRACT:** We have developed the means to simultaneously measure the physical size and count catecholamine molecules in individual nanometer transmitter vesicles. This is done by combining resistive pulse (RP) measurements in a nanopore pipet and vesicle impact electrochemical cytometry (VIEC) at an electrode as the vesicle exits the nanopore. Analysis of freshly isolated bovine adrenal vesicles shows that the size and internal catecholamine concentration of vesicles varies with the occurrence of a dense core inside the vesicles. These results might benefit the understanding about the vesicles maturation, especially involving the "sorting by retention" process and concentration increase of intravesicular catecholamine. The methodology is applicable to understanding soft nanoparticle collisions on electrodes, vesicles in exocytosis and phagocytosis, intracellular vesicle transport, and analysis of electroactive drugs in exosomes.

As a crucial organelle to intercellular communication and modulation of above physiological processes, vesicles within multiple cells, like neuronal cells,[1−5] beta cells,[6−10] hormonal cells,[11−15] platelets,[16−18] etc., have been investigated in many aspects. Especially, their involvement in molecular release, exocytosis, has attracted great interest and been extensively studied in recent years owing to its importance in many fields such as neuroscience and diabetes.

In recent years, micro-/nano-electrochemical approaches have been developed to realize the quantitative measurement of intravesicular content and real-time monitoring of their release dynamics.[19−26] Our group developed a new technique, vesicle impact electrochemical cytometry (VIEC),[27−29] providing a highly effective way to quantify the intravesicular electroactive contents, such as catecholamines, inside each single vesicle. However, to the best of our knowledge, the relationship between size and content concentration of individual vesicle, which benefits the deeper understanding of the mechanism of exocytosis, has not yet been disclosed.

Although the intravesicular content of individual vesicles can be obtained by VIEC, it is currently not possible to measure the size relating to each measured vesicle. There are several effective commercial techniques capable of measuring the size of vesicles, such as transmission electron microscopy (TEM),[30−33] dynamic light scattering (DLS),[34−36] nanoparticle tracking analysis (NTA),[37−39] and even flow cytometry;[40−42] however, some difficulties still exist. For instance, identifying vesicles from complex cell debris or corresponding their signal to the content quantification method, like VIEC, and none of these can currently be used while simultaneously quantifying the vesicle content.

Among those sizing techniques, the resistive pulse (RP) method[43−47] appears compatible with VIEC. With this combination, single vesicles can be manipulated to move one by one across a solid nanopore with varying the pore resistance to measure size, then to impact an electrode surface, release their contents and generate a current transient to quantify the molecular content.

Here we present an effective strategy to combine RP with the VIEC technique to simultaneously measure size and content of isolated nanometer chromaffin vesicles. We then use this to examine the relationship between content concentration and vesicle size.

Periodic pressure applied to the nanopipette is used to eject vesicles in solution having a different osmolality inside compared to outside the tip, and the eluting vesicles are then targeted one at a time onto an electrode. Two circuits are used for synchronous recording of the resistive pulses via the nanopipette tip and current spikes with a carbon fiber microdisk electrode at the VIEC electrode (see Figure 1A and details in Supporting Information (SI)). A periodic measurement cycle is used. Application of a pressure pulse (0.5−1 s) is first used to push out a single vesicle and push away nearby bath solution (LO in Figure 1A,C). The ejected solution surrounding the vesicle (HO in Figure 1A,C) has osmolality close to that of the intravesicular lumen to avoid swelling and breaking of vesicles prior to ejection. In the second step, the pressure is stopped (3−5 s) so the external bath solution, whose osmolality is lower than the intravesicular solution, will return to the electrode surface, pushing back the vesicle solution into the nanopipette by capillary force to stop new particles from flowing out. Vesicles that attach to the

Received: December 8, 2019
Published: February 18, 2020





https://dx.doi.org/10.1021/jacs.9b13221
J. Am. Chem. Soc. 2020, 142, 4093−4097

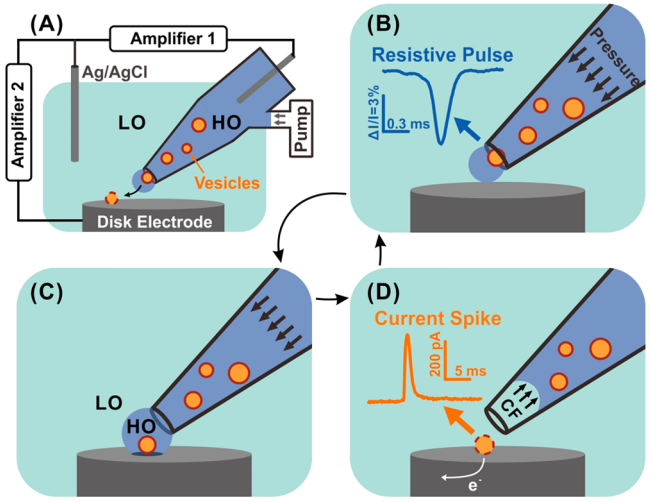


**Figure 1.** Schematic of RP-VIEC. (A) electrode configuration for RP-VIEC. Amplifier 1 records the RP at a potential of +13 mV vs Ag/AgCl reference electrode. Amplifier 2 records the current spike for VIEC with electrode potential set to +700 mV vs the same reference electrode. (B–D) Schematics showing a cycle induced by periodic pressure: (B) Pressure is applied to push a vesicle across the nanopore and generate an RP signal. (C) The vesicle attaches on the electrode surface and is surrounded by the outflowing buffer with relatively high osmolality (similar to vesicular lumen). LO, low osmolarity; HO, high osmolality. (D) Suspended pressure results in capillary force (CF) stopping solution outflow. The vesicle on the surface opens by electroporation aided by the relatively low osmolarity of the surrounding solution. Electroactive content of the vesicle is electrooxidized and generates a current spike.

electrode break in a short time (96% of 340 vesicles open in less than 5 s, see SI, Figure S1). This is facilitated by the low osmolality, and all the intravesicular catecholamine electrooxidized at the electrode producing current spikes that can be quantified. When there is only one resistive pulse and only one current spike appears in one cycle, they can be assumed to come from the same vesicle (this occurs in 3–7% of pulses empirically; the vesicle concentration is kept low enough to minimize pulses ejecting more than one vesicle). This is discussed further in the SI (see Figure S2).

Chromaffin vesicles, containing catecholamines, were isolated from bovine adrenal glands and were investigated after pretreatment through this strategy. After subtracting the baselines in both traces, some examples showing the spike following the RP are observed (see Figure 2 and SI, Figure S2). To analyze the RP signal, an algorithm[48] was adopted, and it was used to effectively relate the magnitude of the RP signal to the ratio of the radius of the vesicular particle and the nanopore (see details in SI and Figure S4).

After estimating the pore size by scanning electron microscopy (see an example in SI, Figure S5), the size of individual vesicle can be calculated. The catecholamine content was evaluated by VIEC as described in the SI. Further, the concentration ($C$) was calculated by use of individual vesicle radius ($r$) and vesicular catecholamine content in moles ($N$), using the equation:

$$C = \frac{3N}{4N_A \pi r^3} \quad (1)$$

where $N_A$ is Avogadro's number ($6.022 \times 10^{23}$ mol$^{-1}$). We collected 278 simultaneous measurements of vesicular

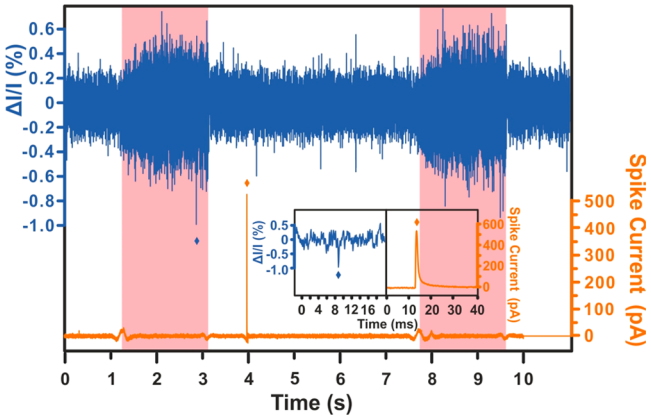


**Figure 2.** An example an RP vs VIEC signal. The blue trace is the RP recording and it is shown in the form of normalized current decline, and the orange trace is VIEC and shown as spike current. The data from both traces are processed (raw traces in SI, Figure S3). The inset is the magnification of both signals, including a RP signal and its following VIEC signal (marked with an asterisk for each). The pink zones indicate when the pressure is applied, and white zones indicate when it is stopped. RP spikes in the white zone without corresponding VIEC signals are likely due to dust or other particles that do not impact or create a signal at the electrode and so are not considered.

catecholamine content and vesicle radius, and these are plotted in Figure 3 with their respective histograms. The median of vesicle radius is 216 nm, with $2.64 \times 10^6$ molecules and a calculated concentration of 0.101 M (see the histogram of concentration in SI, Figure S6).

Notably, our results appear to provide insight into the quantitative aspect of vesicle maturation, especially regarding the dense core within vesicles. The vesicular dense core,

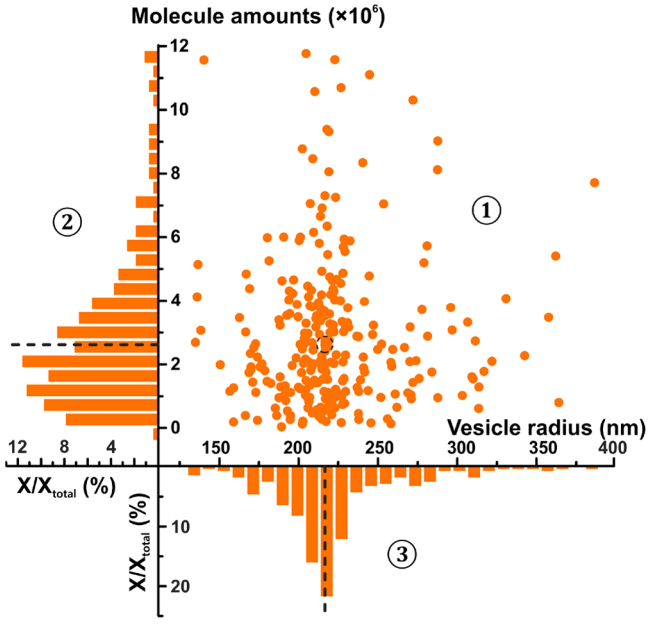


**Figure 3.** Statistical distribution of vesicle content versus radius of each individual recorded chromaffin vesicle. The relationship between content versus radius is shown in a scatter plot in part ①; the normalized frequency histograms of content are depicted in part ② and vesicle radius in part ③. Parts ① and ② share the $Y$-axis, and parts ① and ③ share the $X$-axis. The dotted lines and circle indicate the median position for each parameter measured.



https://dx.doi.org/10.1021/jacs.9b13221
J. Am. Chem. Soc. 2020, 142, 4093–4097

consisting of polyanionic protein, is thought to largely complex the catecholamines via electrostatic interaction. We sorted the current transients for VIEC of single vesicles by curve fitting the falling phase (after the peak) of the current spikes.[49] The previous theoretical analysis considered only vesicles with dense cores and yet provided a potential framework to explain events that have single versus multiple exponential declines on the falling part of the event. However, as exocytosis is partial,[2,50−52] this means that release is more complex with single exponential events for release from the spaces vs double exponential events from both the spaces and the dense core in the vesicle. In VIEC where the entire vesicle content is measured, we interpret events with single exponential to represent immature vesicles (NDCVs). If the falling phase is fit by a single exponential decline, we interpret this to indicate that the vesicle does not have a protein dense core, and a double exponential fit reflects the existence of a dense core. We then classified all the simultaneous measurements of catecholamine amount (VIEC) and radius (RP) for vesicles into two groups via a fit of one or two exponentials in the respective current spike. With the assumptions above, this allowed us to divide spikes into those having dense cores (DCV, $n$ = 150) and those apparently without dense cores (NDCV, $n$ = 128). In SI, Figure S7, we show the statistical distribution of the vesicle radii and their catecholamine concentrations for both groups. The median concentration of the DCVs is higher than the NDCVs (0.116 M for DCVs versus 0.062 M for NDCVs, $P$ < 0.01, see the inset in SI, Figure S7②), and the median radius of the DCVs is slightly smaller (216 nm for DCVs versus 218 nm for NDCVs, $P$ < 0.1, see the inset in SI, Figure S7③). Also, the median catecholamine numbers are higher for DCVs ($2.8 \times 10^6$ molecules for DCVs versus $2.1 \times 10^6$ molecules for NDCVs, $P$ < 0.01, see SI, Figure S8).

DCVs are usually considered to be more mature vesicles than NDCVs. Our results provide a novel perspective on the hypothetical process called "sorting by retention" for protein recycling (see SI, Figure S9)[53,54] during vesicle maturation. Briefly, after being formed from the *trans*-Golgi network and homotypic fusion, immature vesicles will expel those proteins not destined for mature vesicles via budding off of small clathrin-coated vesicles, possibly leading to a slight decrease in vesicle size. Subsequently, the following condensation and acidification of the vesicular lumen will increase the concentration of intravesicular catecholamines as the dense core is formed.[55−57] Our data are consistent with this process.

In conclusion, our work presents an effective approach to simultaneously correlate the size of an individual chromaffin vesicle and its intravesicular catecholamine content. By use of the resistive pulses caused by a vesicle exiting a nanopore and then capturing the vesicle on an electrode for analysis, the RP-VIEC approach allows us to examine individual vesicles for size and molecular content and to examine the distribution of these two parameters. Furthermore, with vesicle size and content, we can calculate catecholamine concentration in each vesicle separately and examine its variation, whereas this was only possible for populations of vesicles in previous experiments. Analysis of isolated chromaffin vesicles indicates size and catecholamine concentration are different between DCVs and NDCVs. Thus, this might be a means to provide quantitative information about the vesicle maturation process. The strategy presented here should benefit further investigation of vesicle-related physiology processes, including exocytosis, phagocytosis, intracellular vesicle transport, as well as analysis of electroactive drugs in exosomes.

## ■ ASSOCIATED CONTENT

### Supporting Information

The Supporting Information is available free of charge at https://pubs.acs.org/doi/10.1021/jacs.9b13221.

Experimental details and procedures for vesicles isolation, resistive pulse recording, electrochemical measurements, and data processing (PDF)

## ■ AUTHOR INFORMATION


### Corresponding Author

**Andrew G. Ewing** − *Department of Chemistry and Molecular Biology, University of Gothenburg SE-412 96 Gothenburg, Sweden;* orcid.org/0000-0002-2084-0133; Email: andrew.ewing@chem.gu.se

### Authors

**Xin-Wei Zhang** − *Department of Chemistry and Molecular Biology, University of Gothenburg SE-412 96 Gothenburg, Sweden*

**Amir Hatamie** − *Department of Chemistry and Molecular Biology, University of Gothenburg SE-412 96 Gothenburg, Sweden*

Complete contact information is available at: https://pubs.acs.org/10.1021/jacs.9b13221


### Notes

The authors declare no competing financial interest.

## ■ ACKNOWLEDGMENTS

We acknowledge funding from the European Research Council (Advanced Grant), the Knut and Alice Wallenberg Foundation, the Swedish Research Council (VR), and the National Institutes of Health. We acknowledge Dalsjöfors Kött AB (Dalsjöfors, Sweden) for donation of bovine adrenal glands. We also acknowledge Prof. Róbert E. Gyurcsányi and Dr. István Makra for their kindly assistance on the resistive pulse algorithm.

## ■ REFERENCES


(1) Dürst, C. D.; Wiegert, J. S.; Helassa, N.; Kerruth, S.; Coates, C.; Schulze, C.; Geeves, M. A.; Török, K.; Oertner, T. G. High-Speed Imaging of Glutamate Release with Genetically Encoded Sensors. *Nat. Protoc.* **2019**, *14*, 1401−1424.

(2) Phan, N. T. N.; Li, X.; Ewing, A. G. Measuring Synaptic Vesicles Using Cellular Electrochemistry and Nanoscale Molecular Imaging. *Nat. Rev. Chem.* **2017**, *1*, 0048.

(3) Rizo, J.; Xu, J. The Synaptic Vesicle Release Machinery. *Annu. Rev. Biophys.* **2015**, *44*, 339−367.

(4) Liu, C.; Kaeser, P. S. Mechanisms and Regulation of Dopamine Release. *Curr. Opin. Neurobiol.* **2019**, *57*, 46−53.

(5) Anantharam, A.; Kreutzberger, A. J. B. Unraveling the Mechanisms of Calcium-Dependent Secretion. *J. Gen. Physiol.* **2019**, *151*, 417−434.

(6) Vakilian, M.; Tahamtani, Y.; Ghaedi, K. A Review On Insulin Trafficking and Exocytosis. *Gene* **2019**, *706*, 52−61.

(7) Guest, P. C. Biogenesis of the Insulin Secretory Granule in Health and Disease. *Adv. Exp. Med. Biol.* **2019**, *1134*, 17−32.

(8) Frank, J. A.; Broichhagen, J.; Yushchenko, D. A.; Trauner, D.; Schultz, C.; Hodson, D. J. Optical Tools for Understanding the Complexity of B-Cell Signalling and Insulin Release. *Nat. Rev. Endocrinol.* **2018**, *14*, 721−737.

(9) Rorsman, P.; Ashcroft, F. M. Pancreatic β-Cell Electrical Activity and Insulin Secretion: Of Mice and Men. *Physiol. Rev.* **2018**, *98*, 117−214.
(10) Hastoy, B.; Clark, A.; Rorsman, P.; Lang, J. Fusion Pore in Exocytosis: More than an Exit Gate? Aβ-Cell Perspective. *Cell Calcium* **2017**, *68*, 45−61.
(11) Thorn, P.; Zorec, R.; Rettig, J.; Keating, D. J. Exocytosis in Non-Neuronal Cells. *J. Neurochem.* **2016**, *137*, 849−859.
(12) Maj, M.; Wagner, L.; Tretter, V. 20 Years of Secretagogin: Exocytosis and Beyond. *Front. Mol. Neurosci.* **2019**, *12*, 29.
(13) Wightman, R. M.; Domínguez, N.; Borges, R. How Intravesicular Composition Affects Exocytosis. *Pfluegers Arch.* **2018**, *470*, 135−141.
(14) Marengo, F. D.; Cárdenas, A. M. How Does the Stimulus Define Exocytosis in Adrenal Chromaffin Cells? *Pfluegers Arch.* **2018**, *470*, 155−167.
(15) Albillos, A.; Dernick, G.; Horstmann, H.; Almers, W.; Alvarez de Toledo, G.; Lindau, M. The Exocytotic Event in Chromaffin Cells Revealed by Patch Amperometry. *Nature* **1997**, *389*, 509−512.
(16) Sharda, A.; Flaumenhaft, R. The Life Cycle of Platelet Granules. *F1000Research* **2018**, *7*, 236.
(17) Yadav, S.; Storrie, B. The Cellular Basis of Platelet Secretion: Emerging Structure/Function Relationships. *Platelets* **2017**, *28*, 108−118.
(18) Manne, B. K.; Xiang, S. C.; Rondina, M. T. Platelet Secretion in Inflammatory and Infectious Diseases. *Platelets* **2017**, *28*, 155−164.
(19) Qi, C.; Sha, Z.; Li, X. Electrochemical Analysis of Single Neuronal Vesicles. *Chin. J. Anal. Chem.* **2019**, *47*, 1502−1511.
(20) Hu, K.; Li, Y.; Rotenberg, S. A.; Amatore, C.; Mirkin, M. V. Electrochemical Measurements of Reactive Oxygen and Nitrogen Species inside Single Phagolysosomes of Living Macrophages. *J. Am. Chem. Soc.* **2019**, *141*, 4564−4568.
(21) White, K. A.; Mulberry, G.; Smith, J.; Lindau, M.; Minch, B. A.; Sugaya, K.; Kim, B. N. Single-Cell Recording of Vesicle Release From Human Neuroblastoma Cells Using 1024-ch Monolithic CMOS Bioelectronics. *IEEE T. Biomed. Circ. S.* **2018**, *12*, 1345−1355.
(22) Barlow, S. T.; Louie, M.; Hao, R.; Defnet, P. A.; Zhang, B. Electrodeposited Gold On Carbon-Fiber Microelectrodes for Enhancing Amperometric Detection of Dopamine Release From Pheochromocytoma Cells. *Anal. Chem.* **2018**, *90*, 10049−10055.
(23) Li, X.; Majdi, S.; Dunevall, J.; Fathali, H.; Ewing, A. G. Quantitative Measurement of Transmitters in Individual Vesicles in the Cytoplasm of Single Cells with Nanotip Electrodes. *Angew. Chem., Int. Ed.* **2015**, *54*, 11978−11982.
(24) Liu, Y.; Li, M.; Zhang, F.; Zhu, A.; Shi, G. Development of Au Disk Nanoelectrode Down to 3 Nm in Radius for Detection of Dopamine Release From a Single Cell. *Anal. Chem.* **2015**, *87*, 5531−5538.
(25) Zhang, X.; Oleinick, A.; Jiang, H.; Liao, Q.; Qiu, Q.; Svir, I.; Liu, Y.; Amatore, C.; Huang, W. Electrochemical Monitoring of ROS/RNS Homeostasis within Individual Phagolysosomes Inside Single Macrophages. *Angew. Chem., Int. Ed.* **2019**, *58*, 7753−7756.
(26) Shen, M.; Qu, Z.; DesLaurier, J.; Welle, T. M.; Sweedler, J. V.; Chen, R. Single Synaptic Observation of Cholinergic Neurotransmission on Living Neurons: Concentration and Dynamics. *J. Am. Chem. Soc.* **2018**, *140*, 7764−7768.
(27) Li, X.; Dunevall, J.; Ren, L.; Ewing, A. G. Mechanistic Aspects of Vesicle Opening during Analysis with Vesicle Impact Electrochemical Cytometry. *Anal. Chem.* **2017**, *89*, 9416−9423.
(28) Lovrić, J.; Najafinobar, N.; Dunevall, J.; Majdi, S.; Svir, I.; Oleinick, A.; Amatore, C.; Ewing, A. G. On the Mechanism of Electrochemical Vesicle Cytometry: Chromaffin Cell Vesicles and Liposomes. *Faraday Discuss.* **2016**, *193*, 65−79.
(29) Dunevall, J.; Fathali, H.; Najafinobar, N.; Lovric, J.; Wigström, J.; Cans, A.; Ewing, A. G. Characterizing the Catecholamine Content of Single Mammalian Vesicles by Collision−Adsorption Events at an Electrode. *J. Am. Chem. Soc.* **2015**, *137*, 4344−4346.
(30) Berclaz, N.; Müller, M.; Walde, P.; Luisi, P. L. Growth and Transformation of Vesicles Studied by Ferritin Labeling and Cryotransmission Electron Microscopy. *J. Phys. Chem. B* **2001**, *105*, 1056−1064.
(31) Crawford, A. R.; Smith, A. J.; Hatch, V. C.; Oude Elferink, R. P.; Borst, P.; Crawford, J. M. Hepatic Secretion of Phospholipid Vesicles in the Mouse Critically Depends On Mdr2 Or MDR3 P-glycoprotein Expression. Visualization by Electron Microscopy. *J. Clin. Invest.* **1997**, *100*, 2562−2567.
(32) Fertig, E. T.; Gherghiceanu, M.; Popescu, L. M. Extracellular Vesicles Release by Cardiac Telocytes: Electron Microscopy and Electron Tomography. *J. Cell. Mol. Med.* **2014**, *18*, 1938−1943.
(33) Coldren, B.; van Zanten, R.; Mackel, M. J.; Zasadzinski, J. A.; Jung, H. From Vesicle Size Distributions to Bilayer Elasticity via Cryo-Transmission and Freeze-Fracture Electron Microscopy. *Langmuir* **2003**, *19*, 5632−5639.
(34) Hallett, F. R.; Watton, J.; Krygsman, P. Vesicle Sizing: Number Distributions by Dynamic Light Scattering. *Biophys. J.* **1991**, *59*, 357−362.
(35) Pencer, J.; Hallett, F. R. Effects of Vesicle Size and Shape on Static and Dynamic Light Scattering Measurements. *Langmuir* **2003**, *19*, 7488−7497.
(36) Day, E. P.; Ho, J. T.; Kunze, R. K.; Sun, S. T. Dynamic Light Scattering Study of Calcium-Induced Fusion in Phospholipid Vesicles. *Biochim. Biophys. Acta, Biomembr.* **1977**, *470*, 503−508.
(37) Pencer, J.; Hallett, F. R. Effects of Vesicle Size and Shape On Static and Dynamic Light Scattering Measurements. *Langmuir* **2003**, *19*, 7488−7497.
(38) Dragovic, R. A.; Southcombe, J. H.; Tannetta, D. S.; Redman, C. W. G.; Sargent, I. L. Multicolor Flow Cytometry and Nanoparticle Tracking Analysis of Extracellular Vesicles in the Plasma of Normal Pregnant and Pre-Eclamptic Women. *Biol. Reprod.* **2013**, *89*, 1−12.
(39) Vestad, B.; Llorente, A.; Neurauter, A.; Phuyal, S.; Kierulf, B.; Kierulf, P.; Skotland, T.; Sandvig, K.; Haug, K. B. F.; Øvstebø, R. Size and Concentration Analyses of Extracellular Vesicles by Nanoparticle Tracking Analysis: A Variation Study. *J. Extracell. Vesicles* **2017**, *6*, 1344087.
(40) van der Vlist, E. J.; Nolte-'T Hoen, E. N. M.; Stoorvogel, W.; Arkesteijn, G. J. A.; Wauben, M. H. M. Fluorescent Labeling of Nano-Sized Vesicles Released by Cells and Subsequent Quantitative and Qualitative Analysis by High-Resolution Flow Cytometry. *Nat. Protoc.* **2012**, *7*, 1311−1326.
(41) Stoner, S. A.; Duggan, E.; Condello, D.; Guerrero, A.; Turk, J. R.; Narayanan, P. K.; Nolan, J. P. High Sensitivity Flow Cytometry of Membrane Vesicles. *Cytometry, Part A* **2016**, *89*, 196−206.
(42) Morales-Kastresana, A.; Telford, B.; Musich, T. A.; McKinnon, K.; Clayborne, C.; Braig, Z.; Rosner, A.; Demberg, T.; Watson, D. C.; Karpova, T. S.; Freeman, G. J.; DeKruyff, R. H.; Pavlakis, G. N.; Terabe, M.; Robert-Guroff, M.; Berzofsky, J. A.; Jones, J. C. Labeling Extracellular Vesicles for Nanoscale Flow Cytometry. *Sci. Rep.* **2017**, *7*, 1878.
(43) Bayley, H.; Martin, C. R. Resistive-Pulse Sensing From Microbes to Molecules. *Chem. Rev.* **2000**, *100*, 2575−2594.
(44) van der Pol, E.; Coumans, F.; Varga, Z.; Krumrey, M.; Nieuwland, R. Innovation in Detection of Microparticles and Exosomes. *J. Thromb. Haemostasis* **2013**, *11*, 36−45.
(45) Blundell, E. L. C. J.; Mayne, L. J.; Billinge, E. R.; Platt, M. Emergence of Tunable Resistive Pulse Sensing as a Biosensor. *Anal. Methods* **2015**, *7*, 7055−7066.
(46) Pan, R.; Hu, K.; Jiang, D.; Samuni, U.; Mirkin, M. V. Electrochemical Resistive-Pulse Sensing. *J. Am. Chem. Soc.* **2019**, *141*, 19555−19559.
(47) Liu, Y.; Xu, C.; Yu, P.; Chen, X.; Wang, J.; Mao, L. Counting and Sizing of Single Vesicles/Liposomes by Electrochemical Events. *ChemElectroChem* **2018**, *5*, 2954−2962.
(48) Terejánszky, P.; Makra, I.; Fürjes, P.; Gyurcsányi, R. E. Calibration-Less Sizing and Quantitation of Polymeric Nanoparticles and Viruses with Quartz Nanopipets. *Anal. Chem.* **2014**, *86*, 4688−4697.
(49) Oleinick, A.; Hu, R.; Ren, B.; Tian, Z.; Svir, I.; Amatore, C. Theoretical Model of Neurotransmitter Release during in Vivo


https://dx.doi.org/10.1021/jacs.9b13221
J. Am. Chem. Soc. 2020, 142, 4093−4097

Vesicular Exocytosis Based on a Grainy Biphasic Nano-Structuration of Chromogranins within Dense Core Matrixes. *J. Electrochem. Soc.* **2016**, *163*, H3014−H3024.
(50) Wu, Q.; Zhang, Q.; Liu, B.; Li, Y.; Wu, X.; Kuo, S.; Zheng, L.; Wang, C.; Zhu, F.; Zhou, Z. Dynamin 1 Restrains Vesicular Release to a Subquantal Mode in Mammalian Adrenal Chromaffin Cells. *J. Neurosci.* **2019**, *39*, 199−211.
(51) Li, X.; Dunevall, J.; Ewing, A. G. Quantitative Chemical Measurements of Vesicular Transmitters with Electrochemical Cytometry. *Acc. Chem. Res.* **2016**, *49*, 2347−2354.
(52) Shin, W.; Ge, L.; Arpino, G.; Villarreal, S. A.; Hamid, E.; Liu, H.; Zhao, W.; Wen, P. J.; Chiang, H.; Wu, L. Visualization of Membrane Pore in Live Cells Reveals a Dynamic-Pore Theory Governing Fusion and Endocytosis. *Cell* **2018**, *173*, 934−945 e12.
(53) Tooze, S. A. Biogenesis of Secretory Granules in the trans-Golgi Network of Neuroendocrine and Endocrine Cells. *Biochim. Biophys. Acta, Mol. Cell Res.* **1998**, *1404*, 231−244.
(54) Arvan, P.; Castle, D. Sorting and Storage During Secretory Granule Biogenesis: Looking Backward and Looking Forward. *Biochem. J.* **1998**, *332*, 593−610.
(55) Myers, M.; Forgac, M. Mechanism and Function of Vacuolar Acidification. *Physiology* **1993**, *8*, 24−29.
(56) Urbé, S.; Dittié, A. S.; Tooze, S. A. PH-dependent Processing of Secretogranin II by the Endopeptidase PC2 in Isolated Immature Secretory Granules. *Biochem. J.* **1997**, *321*, 65−74.
(57) Johnson, R. G. J. Accumulation of Biological Amines Into Chromaffin Granules: A Model for Hormone and Neurotransmitter Transport. *Physiol. Rev.* **1988**, *68*, 232−307.



https://dx.doi.org/10.1021/jacs.9b13221
*J. Am. Chem. Soc.* 2020, 142, 4093−4097